

AD-A074 184

OKLAHOMA UNIV NORMAN SCHOOL OF AEROSPACE MECHANICAL --ETC F/6 12/1
FINITE-ELEMENT ANALYSIS OF LAMINATED BIMODULUS COMPOSITE-MATERI--ETC(U)
AUG 79 J N REDDY, W C CHAO
OU-AMNE-79-18

N00014-78-C-0647

NL

UNCLASSIFIED

| OF |
ADA
074184

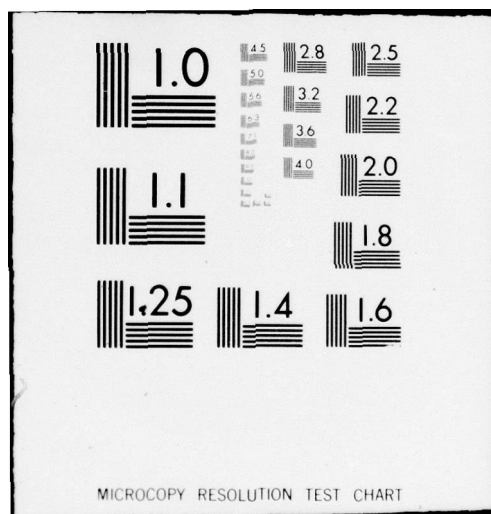


END

DATE
FILMED

10-79

DDC



AD A074184

LEVEL

Department of the Navy
OFFICE OF NAVAL RESEARCH
Structural Mechanics Program
Arlington, Virginia 22217

Contract N00014-78-C-0647
Project NR 064-609
Technical Report No. 7

Report OU-AMNE-79-18, TR-7

FINITE-ELEMENT ANALYSIS OF LAMINATED
BIMODULUS COMPOSITE-MATERIAL PLATES

by

J.N./REDDY and W.C./CHAO

August 1979

DDC FILE COPY

School of Aerospace, Mechanical and Nuclear Engineering
University of Oklahoma
Norman, Oklahoma 73019

Approved for public release; distribution unlimited

400 H98

20 09 18 133

FINITE-ELEMENT ANALYSIS OF LAMINATED
BIMODULUS COMPOSITE-MATERIAL PLATES

J.N. REDDY and W.C. CHAO

School of Aerospace, Mechanical and Nuclear Engineering
The University of Oklahoma, Norman, OK 73019

Abstract - Finite element analysis of the equations governing the small-deflection elastic behavior of thin plates laminated of anisotropic bimodulus materials (which have different elastic stiffnesses depending upon the sign of the fiber-direction strain) is presented. Single-layer and two-layer cross-ply, simply-supported rectangular plates subjected to sinusoidally distributed normal pressure and uniformly distributed normal pressure are analyzed. For the sinusoidally loaded case, the finite element solutions are gratifyingly close to the exact closed-form solutions.

NOMENCLATURE

- A_{ij} = stretching stiffness
 a, b = dimensions of plate in x and y directions
 B_{ij} = bending-stretching stiffness
 c = a/b
 D_{ij} = bending stiffness
 $E_{11}^c, E_{11}^t, \text{etc.}$ = respective compressive and tensile Young's moduli for orthotropic bimodulus material (without subscripts for isotropic bimodulus material)
 F_i = finite-element force components

- G_{12}^C, G_{12}^t , etc. = shear moduli for orthotropic bimodulus material
 h = total thickness of plate
 $K = E_{22}^C W h^3 / q a^4$
 K_{ij} = stiffness coefficients in the finite-element formulation
 M_i, N_i = stress couples and stress resultants ($i=1,2,6$)
 Q_{ijkl} = plane-stress-reduced stiffnesses for orthotropic material
 q = normal pressure
 q_0 = maximum normal pressure
 R = midsurface of the plate
 S_{ij}^{en} = finite-element matrix coefficients
 u, v, w = displacements in x, y, z directions
 x, y, z = plate coordinates in longitudinal, transverse, and downward thickness directions
 $Z_x, Z_y = z_{nx}/h, z_{ny}/h$
 z_{nx}, z_{ny} = neutral-surface positions associated with $\epsilon_x = 0$ and $\epsilon_y = 0$
 α_1, α_2 = penalty parameters
 ϵ_f^l = fiber-direction strain in l -th layer
 ϵ_j = strain component at arbitrary location (x, y, z) , ($j=1,2,6$)
 ϕ_i = finite-element interpolation functions
 σ_j = stress component ($j=1,2,6$)
 ν_{12}^t, ν_{12}^C = principal Poisson's ratios for orthotropic bimodulus material
 θ_i = angle between fiber direction and plate reference direction (x axis)
 θ_x, θ_y = slopes, $\partial w / \partial x, \partial w / \partial y$ (and slope functions in the YNS theory)

1. INTRODUCTION

Fiber-reinforced composite materials are finding widespread use in many engineering structures. This is primarily due to their high stiffness-

to-weight ratio, and anisotropic material properties that can be tailored through variation of the fiber orientation and stacking sequence. Material characterization of composite materials has shown that certain composite materials, known as bimodulus materials, behave differently in simple tension and compression under static loading [1]. The analysis of bimodulus materials is more difficult than that of ordinary materials (i.e., materials whose elastic moduli are the same in tension and compression) since the elastic moduli depend on the sign of the stress, which is unknown a-priori. A plate bent by transverse load experiences both tension and compression, and therefore the analysis of plates made of bimodulus material becomes more difficult.

The first material model appropriate for bimodulus materials is apparently due to Ambartsumyan and Khachatryan [2,3]. There have been only a small number of bimodulus material applications to structural plate problems (see [4-11]). All of these analyses were limited to isotropic materials with different properties in tension and compression. Ambartsumyan [3] and Tabaddor [9] proposed linearized material models for bimodulus anisotropic materials, while Jones and Morgan [10] presented a closed-form solution for cylindrical bending of a thin, cross-ply laminate. More recently, Bert [11] presented a macroscopic material model for bimodulus fiber-reinforced composites. This model was found to agree well with experimental results. A summary of various bimodulus material models can be found in the survey paper of Bert [12]. Using the material model of Bert [11], closed-form solutions have been developed for clamped elliptic plates under uniform loading and simply-supported rectangular plates under sinusoidal loading [13].

| | | |
|--------------------|---------------|--|
| Accession For | RTIS Grant | |
| | DDC TAB | |
| | Unannounced | |
| | Justification | |
| By | | |
| Distribution/ | | |
| Availability Codes | | |
| Avail and/or | | |
| special | | |

The present paper is concerned with the finite-element analysis of thin elastic plates laminated of anisotropic bimodulus materials described by the model of [11]. Numerical results are presented for single-layer and two-layer cross-ply, simply-supported rectangular plates under both sinusoidal loading and uniform loading. Only in the case of sinusoidal loading does a closed-form solution exist [13] for rectangular plates. In this case, the present finite-element solution closely agrees with the exact closed-form solution. Apparently, the present investigation is the first to consider the finite-element analysis of anisotropic bimodulus plates of finite dimensions.

2. THEORY AND FORMULATION

Consider a plate of constant thickness h composed of thin anisotropic layers oriented, generally speaking, at angles $\theta_1, \theta_2, \dots$. The origin of the coordinate system is located within the middle plane (x, y) with the z -axis being normal to the midplane. The material of each layer is assumed to possess a plane of elastic symmetry parallel to the xy -plane. The thin-plate equilibrium equations, in the absence of body forces and body moments, are

$$\frac{\partial N_1}{\partial x} + \frac{\partial N_6}{\partial y} = 0, \quad \frac{\partial N_6}{\partial x} + \frac{\partial N_2}{\partial y} = 0 \quad (2.1)$$

$$\frac{\partial^2 M_1}{\partial x^2} + 2 \frac{\partial^2 M_6}{\partial x \partial y} + \frac{\partial^2 M_2}{\partial y^2} = q$$

where

$$(N_1, N_2, N_6) = \int_{-h/2}^{h/2} (\sigma_1, \sigma_2, \sigma_6) dz, \quad (M_1, M_2, M_6) = \int_{-h/2}^{h/2} (\sigma_1, \sigma_2, \sigma_6) z dz \quad (2.2)$$

All of the symbols have the usual meaning and are defined in the Nomenclature.

In the thin-plate theory (Kirchhoff hypothesis), the strain-displacement relations are given by

$$\epsilon_1 = \frac{\partial u}{\partial x} - z \frac{\partial \theta_x}{\partial x}, \quad \epsilon_2 = \frac{\partial u}{\partial y} - z \frac{\partial \theta_y}{\partial y}, \quad \epsilon_6 = \frac{\partial u}{\partial y} + \frac{\partial v}{\partial x} - z \left(\frac{\partial \theta_x}{\partial y} + \frac{\partial \theta_y}{\partial x} \right) \quad (2.3)$$

where θ_x and θ_y are the slopes,

$$\theta_x - \frac{\partial w}{\partial x} = 0, \quad \theta_y - \frac{\partial w}{\partial y} = 0 \quad (2.4)$$

Equations (2.1)-(2.4) are valid for both ordinary and bimodulus materials. What distinguishes a bimodulus material from an ordinary material are the constitutive relations. Following Bert's [11] fiber-governed macroscopic material model, we assume that there are two symmetric plane-stress reduced stiffness matrices: one when the fibers are in tension along their length and another when they are in compression in the same direction. Then the stress-strain relation for a thin orthotropic bimodulus material may be written as

$$\begin{Bmatrix} \sigma_1 \\ \sigma_2 \\ \sigma_3 \end{Bmatrix} = \begin{bmatrix} Q_{11k\ell} & Q_{12k\ell} & 0 \\ Q_{12k\ell} & Q_{22k\ell} & 0 \\ 0 & 0 & Q_{66k\ell} \end{bmatrix} \begin{Bmatrix} \epsilon_1 \\ \epsilon_2 \\ \epsilon_6 \end{Bmatrix} \quad (2.5)$$

where $Q_{ijk\ell}$ denote the plane-stress-reduced stiffnesses for ℓ -th anisotropic layer in tension ($k=1$) or compression ($k=2$):

$$Q_{ijk\ell} = \begin{cases} Q_{ij1\ell} & \text{if } \epsilon_f^\ell \geq 0 \\ Q_{ij2\ell} & \text{if } \epsilon_f^\ell < 0 \end{cases} \quad (2.6)$$

where ϵ_f^{ℓ} denotes the fiber-direction strain at any arbitrary point in layer, ℓ .

The stretching, bending-stretching coupling, and bending stiffnesses of the bimodulus laminate are defined exactly in the same way as in the case of an ordinary laminate,

$$(A_{ij}, B_{ij}, D_{ij}) = \sum_{\ell=1}^N \left\{ \int_{z_{\ell}}^{z_n} Q_{ij1\ell}(1, z, z^2) dz + \int_{z_n}^{z_{\ell+1}} Q_{ij2\ell}(1, z, z^2) dz \right\} \quad (2.7)$$

where z_n is the distance from the midsurface to the neutral plane (which is unknown a-priori). Note that, in addition to performing the integrations in a piecewise manner from layer to layer, one must take into account the possibility of different properties (tension or compression) within a layer.

For example, in the two-layer, cross-ply case, the coefficients A_{ij} are given by

$$A_{ij} = \int_{-h/2}^{z_{ny}} Q_{ij22} dz + \int_{z_{ny}}^0 Q_{ij12} dz + \int_0^{z_{nx}} Q_{ij21} dz + \int_{z_{nx}}^{h/2} Q_{ij11} dz \quad (2.8)$$

wherein it is assumed that layer, $\ell = 1$ (bottom) occupies the thickness space from $z = 0$ to $z = h/2$ and layer, $\ell = 2$ (top) occupies the thickness space from $z = -h/2$ to $z = 0$ (z is measured positive downward from the midplane). In writing eqns. (2.8) it is assumed that the upper portion of the top layer ($\ell=2$) is in compression ($k=2$) in the fiber direction and that the lower portion of the top layer is in tension ($k=1$), while the portion $z = 0$ to $z = z_{nx}$ of the bottom layer ($\ell=1$) is in compression and the portion $z = z_{nx}$ to $z = h/2$ is in tension. Here z_{nx} and z_{ny} denote neutral-surface positions associated with $\epsilon_x = 0$ and $\epsilon_y = 0$, respectively.

Now the laminate constitutive relations for an arbitrary laminate of anisotropic material are (using eqns. (2.2), and (2.5)),

$$\begin{Bmatrix} N_1 \\ N_2 \\ N_6 \\ M_1 \\ M_2 \\ M_6 \end{Bmatrix} = \begin{bmatrix} A_{11} & & & & & \\ & A_{12} & A_{22} & & & \\ & A_{16} & A_{26} & A_{66} & \text{symmetric} & \\ & B_{11} & B_{12} & B_{16} & D_{11} & \\ & B_{12} & B_{22} & B_{26} & D_{12} & D_{22} \\ & B_{16} & B_{26} & B_{66} & D_{16} & D_{26} & D_{66} \end{bmatrix} \begin{Bmatrix} u_{,x} \\ v_{,y} \\ u_{,y} + v_{,x} \\ -\theta_{x,x} \\ -\theta_{y,y} \\ -(\theta_{x,y} + \theta_{y,x}) \end{Bmatrix} \quad (2.9)$$

Substituting eqns. (2.9) into eqns. (2.1), one obtains the governing equations in terms of the displacements. For the finite-element formulation, we construct the associated functional. The problem of seeking solutions to eqns. (2.7) and (2.9) is equivalent to minimizing the total potential energy,

$$\pi(u, v, w, \theta_x, \theta_y) = \frac{1}{2} \int_{-h/2}^{h/2} \int_R \sigma_i \epsilon_i \, dx dy \, dz + \int_R q w \, dx dy \quad (2.10)$$

subject to the constraints in eqn. (2.4). Note that if θ_x and θ_y are eliminated from eqn. (2.10) using relations (2.4), the resulting total potential energy functional involves the second-order derivatives of the transverse deflection, and consequently imposes severe continuity requirements on the finite-element interpolation functions.

To include the constraint conditions into the variational formulation, we use the penalty-function method (see Reddy [14]). In the penalty method, a constrained minimization problem is replaced by an unconstrained minimization problem whose solution converges to the true solution in the limit certain parameter, called the penalty parameter, approaches the value of

infinity. For details, the reader is referred to the senior author's recent paper [14].

The modified functional to be minimized is given by

$$\pi_p(u, v, w, \theta_x, \theta_y) = \pi(u, v, w, \theta_x, \theta_y) + \int_R [\alpha_1 (\frac{\partial w}{\partial x} - \theta_x) + \alpha_2 (\frac{\partial w}{\partial y} - \theta_y)]^2 dx dy \quad (2.11)$$

where α_1 and α_2 are the penalty parameters whose values are to be preassigned (of the order $10^{12} - 10^{15}$). Generally speaking, the penalty functional π_p approaches π as α_1 and α_2 approach ∞ , and for finite values of α_1 and α_2 , π_p has no physical significance. However, in the case of plates, π_p has a physical significance (only incidental): for the following values of α_1 and α_2 , it corresponds to the functional associated with the Yang, Norris, and Stavsky theory (a generalization of Mindlin's theory for isotropic plates to laminated anisotropic plates) [14]:

$$\alpha_1^2 = k_1^2 \int_{-h/2}^{h/2} Q_{55} dz, \quad \alpha_2^2 = k_2^2 \int_{-h/2}^{h/2} Q_{44} dz, \quad \alpha_1 \alpha_2 = k_1 k_2 \int_{-h/2}^{h/2} Q_{45} dz \quad (2.12)$$

where k_1 and k_2 are the shear correction factors, and θ_x and θ_y are the slope functions of the thick-plate theory (not equal to the slopes of w). Thus (in retrospect only) the Mindlin thick-plate theory can be interpreted as a theory obtained from the thin-plate theory by perturbation; for sufficiently large α 's one recovers the thin-plate theory from the thick-plate theory.

3. FINITE-ELEMENT MODELS

We now construct a finite-element model based on $\pi_p(u, v, w, \theta_x, \theta_y)$. We assume, over each element R_e , the same kind of interpolation for all of the variables,

$$u^e = \sum_i^n u_i^e \phi_i^e, \quad v^e = \sum_i^n v_i^e \phi_i^e, \quad \text{etc.} \quad (n = \text{nodes per element}) \quad (3.1)$$

where ϕ_i^e are the element interpolation (or shape) functions, and u_i^e , and v_i^e are the nodal values of u^e and v^e , respectively. Substituting (3.1) into the first variation of $\pi_p^e(u, v, w, \theta_x, \theta_y)$, and collecting the coefficients of the variations, δu_i , δv_i , etc., we obtain

$$[K^e]\{\Delta^e\} = \{F^e\} \quad (3.2)$$

where $\{\Delta^e\} = \{u^e\} \{v^e\} \{w^e\} \{\theta_x^e\} \{\theta_y^e\}^T$, and the elements $K_{ij}^{\alpha\beta}$ ($\alpha, \beta=1, 2, \dots, 5$; $i, j=1, 2, \dots, n$) of the stiffness matrix are given by

$$K_{ij}^{11} = A_{11} S_{ij}^x + A_{16} (S_{ij}^{xy} + S_{ji}^{xy}) + A_{66} S_{ij}^y$$

$$K_{ij}^{12} = A_{12} S_{ij}^{xy} + A_{16} S_{ij}^x + A_{26} S_{ij}^y + A_{66} S_{ji}^{xy}$$

$$K_{ij}^{14} = B_{11} S_{ij}^x + B_{16} (S_{ij}^{xy} + S_{ji}^{xy}) + B_{66} S_{ij}^y$$

$$K_{ij}^{15} = B_{12} S_{ij}^{xy} + B_{16} S_{ij}^x + B_{26} S_{ij}^y + B_{66} S_{ji}^{xy}$$

$$K_{ij}^{22} = A_{26} (S_{ij}^{xy} + S_{ji}^{xy}) + A_{22} S_{ij}^y + A_{66} S_{ij}^x$$

$$K_{ij}^{24} = B_{16} S_{ij}^x + B_{66} S_{ij}^{xy} + B_{12} S_{ji}^{xy} + B_{26} S_{ij}^y$$

$$K_{ij}^{25} = B_{26} (S_{ij}^{xy} + S_{ji}^{xy}) + B_{66} S_{ij}^x + B_{22} S_{ij}^y$$

$$K_{ij}^{33} = \alpha_1^2 S_{ij}^x + \alpha_2^2 S_{ij}^y + \alpha_1 \alpha_2 (S_{ij}^{xy} + S_{ji}^{xy})$$

$$K_{ij}^{34} = \alpha_1^2 S_{ij}^{x0} + \alpha_1 \alpha_2 S_{ij}^{y0}, \quad K_{ij}^{35} = \alpha_1 \alpha_2 S_{ij}^{x0} + \alpha_2^2 S_{ij}^{y0}$$

$$K_{ij}^{44} = D_{11} S_{ij} + D_{16} (S_{ij}^{xy} + S_{ji}^{xy}) + D_{66} S_{ij}^y + \alpha_1^2 S_{ij}^0$$

$$K_{ij}^{45} = D_{12} S_{ij}^{xy} + D_{66} S_{ji}^{xy} + D_{16} S_{ij}^x + D_{26} S_{ij}^y + \alpha_1 \alpha_2 S_{ij}^0$$

$$K_{ij}^{55} = D_{26} (S_{ij}^{xy} + S_{ji}^{xy}) + D_{66} S_{ij}^x + D_{22} S_{ij}^y + \alpha_2^2 S_{ij}^0$$

$$K_{ij}^{13} = K_{ij}^{23} = 0, \quad S_{ij}^{\xi\eta} = \int_{\Omega} e^{\phi_{i,j} \phi_{j,n}} dx dy, \quad (\xi, \eta = 0, x, y)$$

$$F_i^3 = \int_{\Omega} e^q \phi_i dx dy, \quad F_i^1 = F_i^2 = F_i^4 = F_i^5 = 0$$

The element stiffness matrices are assembled in the usual manner, and boundary conditions of the problem are imposed before solving for $\{\Delta\}$.

In the present study linear ($n=4$) elements of the serendepity family are used. The element stiffness matrices for the linear element are of order 20×20 .

4. NUMERICAL RESULTS

In the following we present numerical results for (a) single-layer, isotropic and orthotropic bimodulus rectangular plates, and (b) two-layer, cross-ply ($0^\circ/90^\circ$), orthotropic bimodulus rectangular plates both with simply-supported edge conditions. A mesh of 5×5 in the quarter plate is employed. The side-to-thickness ratio is taken to be 100. For simply-supported plates under sinusoidal loading, the neutral surfaces are planes and closed-form solutions exist [13].

For single-layer, isotropic bimodulus rectangular plate, approximate solution (Kamiya [7]), and closed-form solutions (Bert [13]) are available. Table 4.1 presents a comparison of dimensionless maximum deflections obtained by various methods for the case of sinusoidal loading. Dimensionless neutral-surface position for the same case are compared in Table 4.2. Numerical results obtained by all of the methods are very close. Note that the location of the neutral surface is independent of the plate aspect ratio.

Table 4.1. Comparison of dimensionless maximum deflections for sinusoidally loaded, simply supported square plate made of isotropic bimodulus materials ($\nu^C=0.20$, $b/h=100$)

| a/b | E^t/E^c | Closed-form solution [13] | Approximate solution [7] | Finite-element solution (present work) | | |
|-----|-----------|---|--------------------------|--|--|--------|
| | | $\bar{w} = w_{\max} E^C h^3 / q_0 a^4 \quad (x=0, y=0)$ | | $\bar{u} = u_{\max} / w_{\max} \quad (y=0, x=a/2)$ | $\bar{v} = v_{\max} / w_{\max} \quad (y=a/2, x=0)$ | |
| 0.5 | 0.5 | 0.007018 | — | 0.006966 | 0.5666 | 0.2832 |
| | 1.0 | 0.004730 | — | 0.004697 | 0.0 | 0.0 |
| | 2.0 | 0.003264 | — | 0.003243 | 0.6441 | 0.3219 |
| 1.0 | 0.5 | 0.04387 | 0.0435 | 0.04351 | 0.2833 | 0.2833 |
| | 1.0 | 0.02956 | — | 0.02933 | 0.0 | 0.0 |
| | 2.0 | 0.02040 | 0.0194 | 0.02024 | 0.3224 | 0.3224 |
| 2.0 | 0.5 | 0.11230 | — | 0.11139 | 0.1417 | 0.2835 |
| | 1.0 | 0.07569 | — | 0.07508 | 0.0 | 0.0 |
| | 2.0 | 0.05223 | — | 0.05182 | 0.1928 | 0.3226 |

Table 4.2. Values of the dimensionless neutral-surface position for the isotropic bimodulus rectangular plate of Table 4.1 ($b/h=100$)

| E^t/E^c | a/b = 0.5 | | a/b = 1.0 | | a/b = 2.0 | |
|-----------|---------------------------|----------------------|---------------------------|----------------------|---------------------------|----------------------|
| | Closed-form solution [13] | Present FEM solution | Closed-form solution [13] | Present FEM solution | Closed-form solution [13] | Present FEM solution |
| 0.5 | - 0.08951 | - 0.08951 | -0.08951 | - 0.08951 | -0.08951 | - 0.08951 |
| 1.0 | 0.0 | 0.0 | 0.0 | 0.0 | 0.0 | 0.0 |
| 2.0 | 0.10188 | 0.10189 | 0.10188 | 0.10189 | 0.10188 | 0.10189 |

For the orthotropic bimodulus plates, the following elastic properties (see Bert [13]) are used:

| 1. <u>Aramid-Rubber</u> | Tensile Properties | Compressive Properties |
|-----------------------------|-----------------------|---------------------------|
| Major Young's modulus (GPa) | 3.5842 | 0.0120 |
| Minor Young's modulus (GPa) | 0.00909 | 0.0120 |
| Major Poisson's ratio | 0.416 | 0.205 |
| Shear modulus (GPa) | 0.0037 | 0.0037 |
| 2. <u>Polyester-Rubber</u> | | |
| Major Young's modulus (GPa) | 0.617 | 0.0369 |
| Minor Young's modulus (GPa) | 0.008 | 0.0106 |
| Major Poisson's ratio | 0.475 | 0.185 |
| Shear modulus (GPa) | 0.00262 | 0.00267 |

Table 4.3 shows the closed-form solutions [13], and the finite-element solutions for dimensionless deflections and neutral-surface locations of single-layer, simply-supported rectangular plate subjected to sinusoidal loading. There is excellent agreement between the closed-form solutions and the finite-element solutions.

Numerical results are presented in Table 4.4 for two-layer, cross-ply laminated plate ($0^\circ/90^\circ$) subjected to sinusoidal loading. Again, the closed-form results and the finite-element results are gratifyingly close for both the deflections and neutral-surface locations (which are independent of x and y).

The example problems considered thus far admit closed-form solutions due to the fact that the neutral-surface locations are constant (i.e., independent of x and y) for the particular geometry, support conditions, and loading considered. For the same geometry (i.e., rectangular) and boundary

Table 4.3. Fiber-direction neutral-surface location and deflections for simply-supported rectangular plate of single-layer (0°) aramid-rubber and polyester-rubber ($b/h = 100$)

| Material | Aspect ratio, $c=a/b$ | $Z_x = z_{nx}/h$ | | $\bar{w} = w_{\max} \frac{E_c h^3}{q_0 b^4}$ | | Finite-element solution | |
|------------------|-----------------------|--------------------------|-------------------------|--|-------------------------|----------------------------------|----------------------------------|
| | | Closed-form solution[13] | Finite-element solution | Closed-form solution[13] | Finite-element solution | $\bar{u}=10^3 u_{\max}/w_{\max}$ | $\bar{v}=10^3 v_{\max}/w_{\max}$ |
| Aramid-Rubber | 0.5 | 0.4457 | 0.4454 | 0.001881 | 0.001875 | 0.2808 | 0.1306 |
| | 0.6 | 0.4457 | 0.4451 | 0.003661 | 0.003640 | 0.2342 | 0.1093 |
| | 0.7 | 0.4457 | 0.4447 | 0.006253 | 0.006211 | 0.2007 | 0.09171 |
| | 0.8 | 0.4444 | 0.4440 | 0.009679 | 0.009605 | 0.1754 | 0.07738 |
| | 0.9 | 0.4444 | 0.4431 | 0.01387 | 0.01376 | 0.1556 | 0.06583 |
| | 1.0 | 0.4424 | 0.4420 | 0.01870 | 0.01854 | 0.1397 | 0.05647 |
| | 1.2 | 0.4398 | 0.4393 | 0.02956 | 0.02928 | 0.1158 | 0.04270 |
| | 1.4 | 0.4368 | 0.4363 | 0.04089 | 0.04049 | 0.09864 | 0.03337 |
| | 1.6 | 0.4334 | 0.4328 | 0.05170 | 0.05120 | 0.08562 | 0.02686 |
| | 1.8 | 0.4298 | 0.4292 | 0.06143 | 0.06085 | 0.07548 | 0.02222 |
| | 2.0 | 0.4260 | 0.4254 | 0.06995 | 0.06931 | 0.06732 | 0.01882 |
| Polyester-Rubber | 0.5 | 0.3040 | 0.3041 | 0.000816 | 0.000821 | 0.1974 | 0.08969 |
| | 0.6 | 0.3040 | 0.3041 | 0.001655 | 0.001656 | 0.1588 | 0.07239 |
| | 0.7 | 0.3040 | 0.3039 | 0.002975 | 0.002968 | 0.1364 | 0.06110 |
| | 0.8 | 0.3040 | 0.3036 | 0.004888 | 0.004866 | 0.1194 | 0.05206 |
| | 0.9 | 0.3040 | 0.3031 | 0.007478 | 0.007434 | 0.1061 | 0.04482 |
| | 1.0 | 0.3027 | 0.3026 | 0.01079 | 0.01071 | 0.09548 | 0.03966 |
| | 1.2 | 0.3014 | 0.3012 | 0.01954 | 0.01935 | 0.07930 | 0.03062 |
| | 1.4 | 0.2998 | 0.2995 | 0.03056 | 0.03021 | 0.06764 | 0.02495 |
| | 1.6 | 0.2979 | 0.2976 | 0.04278 | 0.04224 | 0.05882 | 0.02102 |
| | 1.8 | 0.2958 | 0.2954 | 0.05505 | 0.05431 | 0.05192 | 0.01821 |
| | 2.0 | 0.2936 | 0.2931 | 0.06652 | 0.06560 | 0.04636 | 0.01616 |

Table 4.4. Neutral-surface positions and deflections for simply-supported rectangular plates of cross-ply laminated aramid-rubber and polyester-rubber (sinusoidal loading case).

| Material | Aspect ratio c | Z_x | | Z_y | | $WE_{22}^C h^3/qb^4$ | |
|------------------|------------------|--------------------------|-------------------------|--------------------------|-------------------------|--------------------------|-------------------------|
| | | Closed-form solution[13] | Finite-element solution | Closed-form solution[13] | Finite-element solution | Closed-form solution[13] | Finite-element solution |
| Aramid-Rubber | 0.5 | 0.4438 | 0.4390 | - 0.07137 | - 0.07202 | 0.001808 | 0.001801 |
| | 0.6 | 0.4438 | 0.4419 | - 0.06052 | - 0.06208 | 0.003486 | 0.003464 |
| | 0.7 | 0.4423 | 0.4419 | - 0.05165 | - 0.05302 | 0.005925 | 0.005880 |
| | 0.8 | 0.4413 | 0.4413 | - 0.04489 | - 0.04608 | 0.009162 | 0.009082 |
| | 0.9 | 0.4401 | 0.4404 | - 0.03964 | - 0.04145 | 0.01315 | 0.01303 |
| | 1.0 | 0.4389 | 0.4392 | - 0.03546 | - 0.03712 | 0.01780 | 0.01761 |
| | 1.2 | 0.4362 | 0.4360 | - 0.02925 | - 0.03060 | 0.02838 | 0.02807 |
| | 1.4 | 0.4332 | 0.4334 | - 0.02487 | - 0.02592 | 0.03961 | 0.03917 |
| | 1.6 | 0.4300 | 0.4302 | - 0.02163 | - 0.02295 | 0.05046 | 0.04990 |
| | 1.8 | 0.4265 | 0.4266 | - 0.01917 | - 0.02029 | 0.06032 | 0.05967 |
| | 2.0 | 0.4228 | 0.4229 | - 0.01815 | - 0.01818 | 0.06894 | 0.06826 |
| Polyester-Rubber | 0.5 | 0.3650 | 0.3719 | - 0.1412 | - 0.1310 | 0.001902 | 0.001886 |
| | 0.6 | 0.3650 | 0.3653 | - 0.1244 | - 0.1277 | 0.003672 | 0.003648 |
| | 0.7 | 0.3638 | 0.3642 | - 0.1139 | - 0.1171 | 0.006227 | 0.006175 |
| | 0.8 | 0.3638 | 0.3632 | - 0.1060 | - 0.1085 | 0.009542 | 0.009448 |
| | 0.9 | 0.3622 | 0.3626 | - 0.1003 | - 0.1039 | 0.01348 | 0.01333 |
| | 1.0 | 0.3622 | 0.3618 | - 0.09605 | - 0.09925 | 0.01783 | 0.01762 |
| | 1.2 | 0.3594 | 0.3603 | - 0.09029 | - 0.09415 | 0.02680 | 0.02646 |
| | 1.4 | 0.3573 | 0.3583 | - 0.08670 | - 0.08958 | 0.03497 | 0.03451 |
| | 1.6 | 0.3550 | 0.3560 | - 0.08432 | - 0.08628 | 0.04167 | 0.04112 |
| | 1.8 | 0.3525 | 0.3541 | - 0.08268 | - 0.08070 | 0.04690 | 0.04625 |
| | 2.0 | 0.3498 | 0.3541 | - 0.08150 | - 0.07757 | 0.05090 | 0.05021 |

conditions (i.e., simply-supported), if the loading is changed to that of uniform loading, closed-form solution does not exist. However, the finite-element method can predict the neutral-surface locations (which may now depend on x and y) and deflections.

Table 4.5 shows the nondimensional neutral-surface locations at the center of the plate (i.e., in element 1), and deflections for the problem of Table 4.4., but with uniform loading. The trend and magnitudes of the solutions are similar to those in Table 4.4 for the sinusoidal loading. Table 4.6 shows the nondimensional neutral-surface locations for various elements. It is clear that z_x does not vary much along x or y . However, z_y varies noticeably with y while it is almost constant with respect to x . Also, the locations change with the plate aspect ratio.

As pointed out earlier, the present finite-element formulation is also good for thick plates (i.e., accounts for transverse shear deformation). Representative results are presented to show the effect of the thickness on the neutral-surface locations and deflections (see Reddy and Bert [15]).

Figure 4.1 shows the influence of the aspect ratio (b/a) and side-to-thickness ratio (a/h) on the location of neutral surfaces for a single-layer, orthotropic, bimodulus, simply supported rectangular plate subjected to sinusoidal loading. The following elastic properties are used:

$$E_{11}^t = 3.584 \text{ GPa} , E_{11}^c = 1.792 \text{ GPa} , E_{22}^t = E_{11}^t , E_{22}^c = E_{11}^c$$

$$G_{12}^t = G_{12}^c = 1.27 \text{ GPa} , \nu_{12}^t = \nu_{21}^t = 0.4 , \nu_{12}^c = \nu_{21}^c = 0.2$$

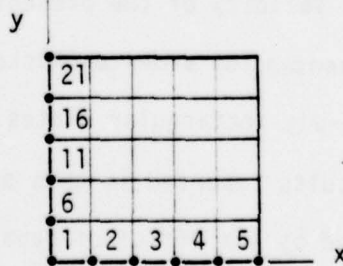
Note that for $b/a = 1$, the neutral surfaces associated with x - and y -directions coincide (i.e., $z_{nx} = z_{ny}$).

Table 4.5. Neutral-surface locations and deflections for simply-supported rectangular plates of cross-ply laminated aramid-rubber and polyester-rubber (uniform-loading case)

| Mat- erial | a/b | Z_x | Z_y | \bar{w} | $\bar{u} \times 10^2$ | $\bar{v} \times 10^2$ |
|------------------|-----|--------|-----------|-----------|-----------------------|-----------------------|
| Aramid-Rubber | 0.5 | 0.4439 | - 0.1141 | 0.00269 | 2.8400 | 0.2744 |
| | 0.6 | 0.4431 | - 0.07943 | 0.00531 | 2.3721 | 0.2161 |
| | 0.7 | 0.4422 | - 0.06152 | 0.00917 | 2.0329 | 0.1781 |
| | 0.8 | 0.4411 | - 0.05067 | 0.01433 | 1.7788 | 0.1513 |
| | 0.9 | 0.4400 | - 0.04328 | 0.02017 | 1.5815 | 0.1314 |
| | 1.0 | 0.4387 | - 0.03787 | 0.02812 | 1.4238 | 0.1161 |
| | 1.2 | 0.4358 | - 0.03037 | 0.04501 | 1.1884 | 0.0940 |
| | 1.4 | 0.4323 | - 0.02529 | 0.06284 | 1.022 | 0.0785 |
| | 1.6 | 0.4281 | - 0.02157 | 0.07989 | 0.8995 | 0.0671 |
| | 1.8 | 0.4232 | - 0.01890 | 0.09516 | 0.8066 | 0.0582 |
| | 2.0 | 0.4174 | - 0.01640 | 0.1082 | 0.7352 | 0.0509 |
| Polyester-Rubber | 0.5 | 0.3659 | - 0.19040 | 0.00287 | 2.3433 | 0.5546 |
| | 0.6 | 0.3648 | - 0.14270 | 0.00568 | 1.9502 | 0.4555 |
| | 0.7 | 0.3639 | - 0.12160 | 0.00976 | 1.6709 | 0.3960 |
| | 0.8 | 0.3631 | - 0.10980 | 0.01507 | 1.4622 | 0.3583 |
| | 0.9 | 0.3622 | - 0.10230 | 0.02137 | 1.3000 | 0.3330 |
| | 1.0 | 0.3612 | - 0.09714 | 0.02832 | 1.1724 | 0.3152 |
| | 1.2 | 0.3590 | - 0.09046 | 0.04258 | 0.9818 | 0.2918 |
| | 1.4 | 0.3564 | - 0.08648 | 0.05544 | 0.8495 | 0.2782 |
| | 1.6 | 0.3533 | - 0.08390 | 0.06580 | 0.7543 | 0.2693 |
| | 1.8 | 0.3493 | - 0.08182 | 0.07361 | 0.6844 | 0.2624 |
| | 2.0 | 0.3445 | - 0.08043 | 0.07927 | 0.6332 | 0.2571 |

Table 4.6. Neutral-surface locations as a function of the element location for simply-supported rectangular plates of cross-ply laminated aramid-rubber and polyester-rubber (uniform-loading case)

| Material | Element No. | a/b = 0.5 | | a/b = 1 | | a/b = 2.0 | |
|------------------|-------------|-----------|------------|---------|------------|-----------|------------|
| | | Z_x | Z_y | Z_x | Z_y | Z_x | Z_y |
| Aramid-Rubber | 1 | 0.44397 | - 0.11414 | 0.44002 | - 0.043286 | 0.41739 | - 0.016405 |
| | 2 | 0.44398 | - 0.11481 | 0.44013 | - 0.043781 | 0.42006 | - 0.017267 |
| | 3 | 0.44401 | - 0.11618 | 0.44033 | - 0.044708 | 0.42421 | - 0.018940 |
| | 4 | 0.44405 | - 0.11792 | 0.44059 | - 0.045820 | 0.42841 | - 0.021052 |
| | 5 | 0.44407 | - 0.11919 | 0.44079 | - 0.046613 | 0.43094 | - 0.022623 |
| | 6 | 0.44325 | - 0.08752 | 0.43947 | - 0.040654 | 0.41693 | - 0.016184 |
| | 11 | 0.44197 | - 0.05971 | 0.43835 | - 0.036348 | 0.41612 | - 0.015769 |
| | 16 | 0.43980 | - 0.04162 | 0.43686 | - 0.031648 | 0.4523 | - 0.015219 |
| | 21 | 0.43796 | - 0.03378 | 0.43572 | - 0.028602 | 0.41463 | - 0.014782 |
| Polyester-Rubber | 1 | 0.36597 | - 0.19040 | 0.36124 | - 0.097142 | 0.34451 | - 0.080437 |
| | 2 | 0.36598 | - 0.19101 | 0.36137 | - 0.097651 | 0.34755 | - 0.081660 |
| | 3 | 0.36600 | - 0.19224 | 0.36161 | - 0.098586 | 0.35165 | - 0.082619 |
| | 4 | 0.36603 | - 0.19386 | 0.36190 | - 0.099683 | 0.35519 | - 0.084542 |
| | 5 | 0.36605 | - 0.19505 | 0.36211 | - 0.010045 | 0.35709 | - 0.086014 |
| | 6 | 0.36526 | - 0.15496 | 0.36101 | - 0.096155 | 0.34431 | - 0.080356 |
| | 11 | 0.36415 | - 0.12374 | 0.36055 | - 0.094110 | 0.34397 | - 0.080201 |
| | 16 | 0.36290 | - 0.10556 | 0.35999 | - 0.091909 | 0.34358 | - 0.079991 |
| | 21 | 0.36199 | - 0.098157 | 0.35961 | - 0.090318 | 0.34331 | - 0.079821 |



Similar results are presented in Figs. 4.2 and 4.3 for a two-layer, cross-ply ($0^\circ/90^\circ$), rectangular plate of aramid-rubber under sinusoidal loading. Note from Fig. 4.2 that the neutral-surface location, Z_x is virtually unchanged for aspect ratios greater than 1, while the neutral-surface location, Z_y , increases proportional to the aspect ratio. It should also be noted that the neutral surfaces do not coincide in the cross-ply case for $b/a = 1$.

Figure 4.4 shows the influence of the aspect ratio, and side-to-thickness ratio on the transverse deflection for the single-layer and two-layer cross-ply plates discussed above. The effect of thickness on the deflection is more pronounced than the effect of the aspect ratio.

5. SUMMARY AND CONCLUSIONS

A penalty finite-element formulation of the equations governing the small deflection elastic behavior of thin plates laminated of anisotropic bimodulus materials is presented. The resulting finite element model is valid for the analysis of thin and moderately thick plates. Single-layer and two-layer cross-ply, simply-supported thin rectangular plates subjected to sinusoidally distributed normal pressure and uniformly distributed normal pressure are analyzed. In the case of sinusoidal loading, the present finite-element solutions agree very closely with the exact closed-form solutions. To illustrate the validity of the present finite element model for thick plates numerical results are presented for side-to-thickness ratio of 10 for single-layer and two-layer cross-ply rectangular plates.

Acknowledgement. The results reported in this paper were obtained during an investigation supported by the Office of Naval Research, Structural Mechanics Program through Contract N00014-78-C-0647. The authors wish to express their sincere thanks to Professor C. W. Bert for helpful discussions.

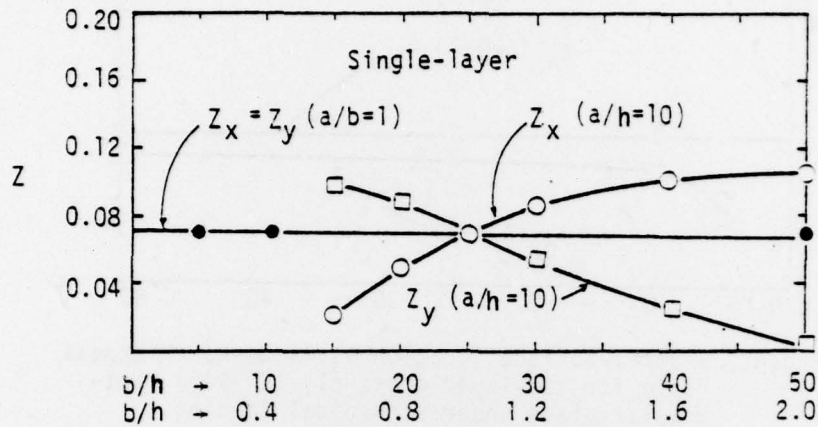


Fig.4.1 Neutral-surface location vs. plate aspect ratio, and side-to-thickness ratio for single-layered rectangular plate under sinusoidal loading.

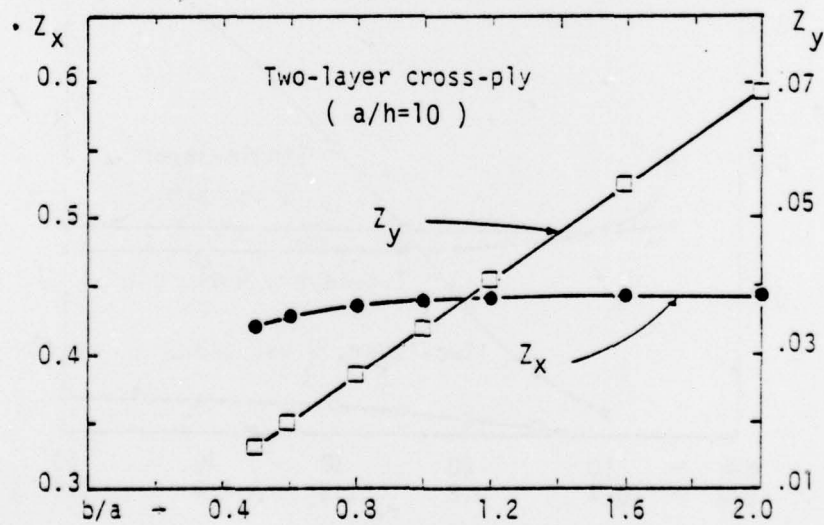


Fig. 4.2 Neutral-surface location vs. plate aspect ratio for two-layer, cross-ply ($0^\circ/90^\circ$) square plate under sinusoidal loading.

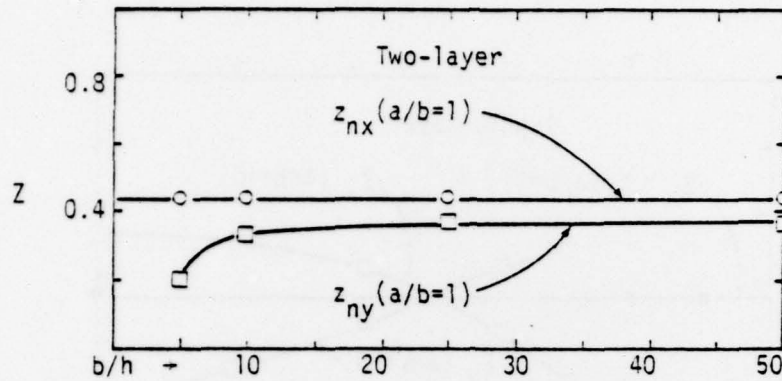


Fig. 4.3 Neutral-surface location vs. side-to-thickness ratio for two-layer cross-ply ($0^\circ/90^\circ$) rectangular plate under sinusoidal loading.

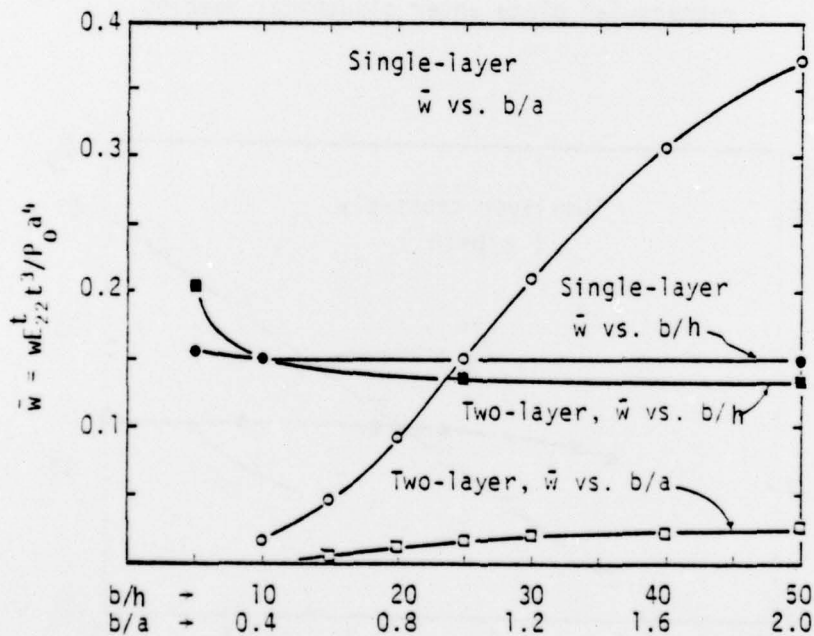


Fig. 4.4 Transverse deflection vs. plate aspect ratio, and side-to-thickness ratio for single-layer and two-layer cross-ply plates under sinusoidal loading.

REFERENCES

1. J. E. Ashton, J. C. Halpin, and P. H. Petit, Primer on Composite Materials: Analysis, Technomic, Stamford, Conn. (1969).
2. S. A. Ambartsumyan and A. A. Khachatryan, "The basic equations of the theory of elasticity for materials with different tensile and compressive strengths," Mechanics of Solids, Vol. 1, No. 2, pp. 29-34 (1966).
3. S. A. Ambartsumyan, "The basic equations and relations of the different-modulus theory of elasticity of an anisotropic body," Mechanics of Solids, Vol. 4, No. 3, pp. 48-56 (1969).
4. S. A. Ambartsumyan, "The axisymmetric problems of a circular cylindrical shell with different stiffness in tension and compression," (in Russian) Izv. Akad. Nauk., SSSR, Mekh., No. 4, pp. 77-85 (1965); English translation, NTIS Document AD 574312 (1967).
5. G. S. Shapiro, "Deformation of bodies with different tensile and compressive strengths," Mechanics of Solids, Vol. 1, No. 2, pp. 85-86 (1966).
6. N. Kamiya, "Large deflection of a different modulus circular plate," Journal of Engineering Materials and Technology, Trans. ASME, Vol. 97H, pp. 52-56 (1975).
7. N. Kamiya, "An energy method applied to large elastic deflection of a thin plate of bimodulus material," Journal of Structural Mechanics, Vol. 3, No. 3, pp. 317-329 (1975).
8. N. Kamiya, "Transverse shear effect in a bimodulus plate," Nuclear Engineering and Design, Vol. 32, No. 3, pp. 351-357 (1975).
9. F. Tabaddor, "Constitutive equations for bimodulus elastic materials," AIAA Journal, Vol. 10, No. 4, pp. 516-518 (1972).
10. R. M. Jones and H. S. Morgan, "Bending and extension of cross-ply laminates with different moduli in tension and compression," Proc. AIAA/ASME/SAE 17th Structures, Structural Dynamics, and Materials Conference, King of Prussia, PA, May 5-7, pp. 158-167 (1976).
11. C. W. Bert, "Models for fibrous composites with different properties in tension and compression," Journal of Engineering Materials and Technology, Trans. ASME, Vol. 99H, No. 4, pp. 344-349 (1977).
12. C. W. Bert, "Recent advances in mathematical modeling of the mechanics of bimodulus, fiber-reinforced composite materials," Recent Advances in Engineering Science (Proc. 15th Annual Meeting, Society of Engineering Science), R. L. Sierakowski (ed.), University of Florida, Gainesville, pp. 101-106 (1978).

13. C. W. Bert, "Classical analyses of laminated bimodulus composite-material plates," University of Oklahoma, School of Aerospace, Mechanical and Nuclear Engineering, Contract N00014-78-C-0647, Report OU-AMNE-79-10A, revised August 1979.
14. J. N. Reddy, "A penalty plate-bending element for the analysis of laminated anisotropic composite plates," University of Oklahoma, School of Aerospace, Mechanical and Nuclear Engineering, Contract N00014-78-C-0647, Report OU-AMNE-79-14, August 1979.
15. J. N. Reddy and C. W. Bert, "Analysis of plates constructed of fiber-reinforced bimodulus material," Symposium on Mechanics of Bimodulus Materials, ASME Winter Annual Meeting, New York, NY, December 1979, to appear.

PREVIOUS REPORTS ON THIS CONTRACT

| <u>Tech. Rept. No.</u> | <u>OU-AMNE Rept. No.</u> | <u>Title of Report</u> | <u>Author</u> |
|----------------------------|------------------------------|--|------------------------------|
| 1 | 79-7 | Mathematical Modeling and Micromechanics of Fiber-Reinforced Bimodulus Composite Materials | C.W. Bert |
| 2 | 79-8 | Analyses of Plates Constructed of Fiber-Reinforced Bimodulus Materials | J.N. Reddy. and C.W. Bert |
| 3 | 79-9 | Finite-Element Analyses of Laminated-Composite-Material Plates | J.N. Reddy |
| 4A | 79-10 | Analyses of Laminated Bimodulus Composite Material Plates | C.W. Bert |
| 5 | 79-11 | Recent Research in Composite and Sandwich Plate Dynamics | C.W. Bert |
| 6 | 79-14 | A Penalty-Plate Bending Element for the Analysis of Laminated Anisotropic Composite Plates | J.N. Reddy |

UNCLASSIFIED

SECURITY CLASSIFICATION OF THIS PAGE (When Data Entered)

| REPORT DOCUMENTATION PAGE | | READ INSTRUCTIONS BEFORE COMPLETING FORM |
|--|-----------------------|---|
| 1. REPORT NUMBER OU-AMNE-79-18 | 2. GOVT ACCESSION NO. | 3. RECIPIENT'S CATALOG NUMBER |
| 4. TITLE (and Subtitle) FINITE-ELEMENT ANALYSIS OF LAMINATED BIMODULUS PLATES | | 5. TYPE OF REPORT & PERIOD COVERED Technical Report No. 7 |
| | | 6. PERFORMING ORG. REPORT NUMBER |
| 7. AUTHOR(s) J. N. Reddy and W. C. Chao | | 8. CONTRACT OR GRANT NUMBER(s) N00014-78-C-0647 |
| 9. PERFORMING ORGANIZATION NAME AND ADDRESS School of Aerospace, Mechanical and Nuclear Engineering University of Oklahoma, Norman, Oklahoma 73019 | | 10. PROGRAM ELEMENT, PROJECT, TASK AREA & WORK UNIT NUMBERS NR 064-609 |
| 11. CONTROLLING OFFICE NAME AND ADDRESS Department of the Navy, Office of Naval Research Structural Mechanics Program (Code 474) Arlington, Virginia 22217 | | 12. REPORT DATE August 1979 |
| | | 13. NUMBER OF PAGES 26 |
| 14. MONITORING AGENCY NAME & ADDRESS (if different from Controlling Office) | | 15. SECURITY CLASS. (of this report) UNCLASSIFIED |
| | | 15a. DECLASSIFICATION/DOWNGRADING SCHEDULE |
| 16. DISTRIBUTION STATEMENT (of this Report) This document has been approved for public release and sale; distribution unlimited. | | |
| 17. DISTRIBUTION STATEMENT (of the abstract entered in Block 20, if different from Report) | | |
| 18. SUPPLEMENTARY NOTES | | |
| 19. KEY WORDS (Continue on reverse side if necessary and identify by block number) Bimodulus materials, fiber-reinforced composites, finite elements, laminated plates, penalty function method, sinusoidal loading, uniform loading. | | |
| 20. ABSTRACT (Continue on reverse side if necessary and identify by block number) Finite-element analysis of the equations governing the small-deflection elastic behavior of thin plates laminated of anisotropic bimodulus materials (which have different elastic stiffnesses depending upon the sign of the fiber-direction strain) is presented. Single-layer and two-layer cross-ply, simply-supported rectangular plates subjected to sinusoidally distributed normal pressure and uniformly distributed normal pressure are analyzed. For the sinusoidally loaded case, the finite-element solutions are gratifyingly close to the exact closed-form solutions. | | |

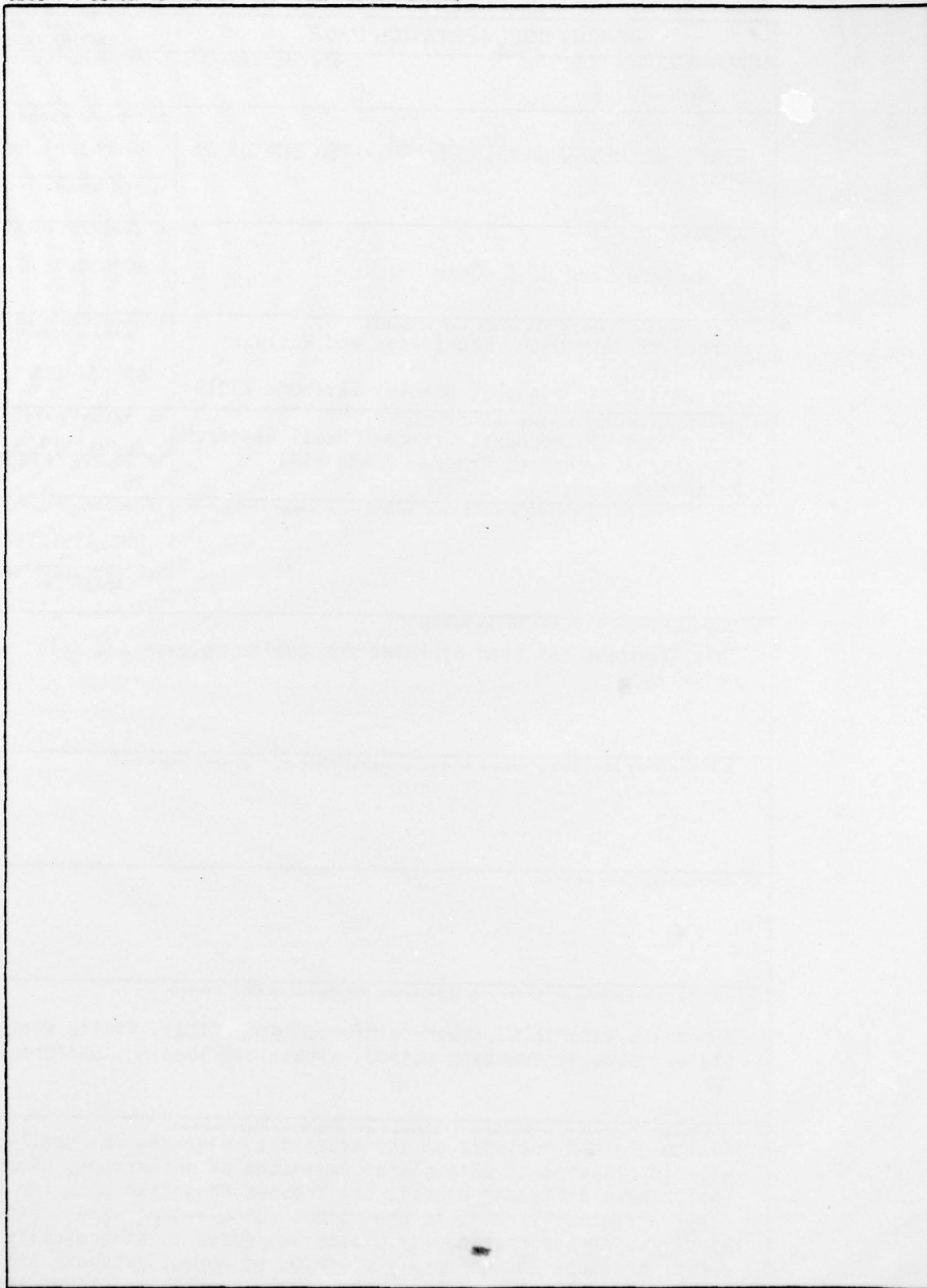
DD FORM 1 JAN 73 1473

EDITION OF 1 NOV 65 IS OBSOLETE
S/N 0102-014-6601

UNCLASSIFIED

SECURITY CLASSIFICATION OF THIS PAGE (When Data Entered)

SECURITY CLASSIFICATION OF THIS PAGE(When Data Entered)



SECURITY CLASSIFICATION OF THIS PAGE(When Data Entered)

